Ecological Indicators 172 (2025) 113263

Contents lists available at ScienceDirect

Ecological Indicators

journal homepage: www.elsevier.com/locate/ecolind

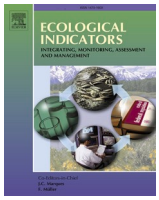

Original Articles

On mature reflection: Ozone damage can be detected in oak trees by hyperspectral reflectance

Anna Lee Jones [a,*], Christian Pfrang [b,c], Felicity Hayes [d], Elizabeth S. Jeffers [a]

[a] Department of Biology, University of Oxford, South Parks Road, Oxford OX1 3SZ, UK
[b] School of Geography, Earth and Environmental Sciences, University of Birmingham, Birmingham B15 2TT, UK
[c] Birmingham Institute of Forest Research, University of Birmingham, Birmingham B15 2TT, UK
[d] UK Centre for Ecology & Hydrology, Environment Centre Wales, Deiniol Road, Bangor LL57 2UW, UK

ARTICLE INFO

Keywords:
Air pollution
Forests
Monitoring
Spectroscopy
Vegetation indices
Forest health

ABSTRACT

At the near-surface, ozone (O_3) is a toxic pollutant which has reached dangerously high concentrations across the world and is predicted to continue to rise. O_3 reduces the growth, productivity and resilience of trees but the extent of O_3 damage to forests is uncertain. To develop a high throughput method of monitoring O_3 damage to forests, we pioneer hyperspectral monitoring of O_3 damage in adult oak trees across a range of naturally occurring O_3 concentrations. Using a machine learning approach, we demonstrate accurate prediction of O_3 exposure of trees from hyperspectral leaf reflectance alone. This method could be used for forest level assessments of O_3 damage. Vegetation indices characterising green reflectance and red-edge track O_3 induced changes in leaf reflectance. Vegetation indices have the potential to scale up O_3 damage monitoring across spatial scales. As O_3 concentrations continue to rise globally, understanding the extent of O_3 damage to forests is crucial to effectively harness the carbon sequestration potential of forests. We demonstrate the exciting potential of spectral monitoring of O_3 damage in mature trees under natural conditions.

1. Introduction

O_3 is highly oxidising, and direct contact with O_3 at the ground level is toxic to both plant and animal life (Donzelli and Suarez-Varela, 2024; Lefohn et al., 2018). Ground-level or tropospheric O_3 is a secondary pollutant formed by sunlight induced reactions of nitrogen oxides and volatile organic compounds (Monks et al., 2015). Tropospheric O_3 concentrations have been increasing since the 1950s when reliable global monitoring began (IPCC, 2023). Despite controls on vehicular emissions of nitrogen oxides, background tropospheric O_3 concentrations are increasing and are predicted to continue to rise for the rest of the century (Christiansen et al., 2022; Cooper et al., 2014; Finch and Palmer, 2020; Griffiths et al., 2021).

When O_3 enters leaves via the stomata, it causes oxidative stress and triggers a range of defence mechanisms (Sandermann, 1996) including the hypersensitive response (Kangasjärvi et al., 2005) and antioxidant synthesis (Sharma and Davis, 1997). In the short term, O_3 exposure induces stomatal closure and a reduction in photosynthetic activity (Hill and Littlefield, 1969). Long-term O_3 exposure results in altered allocation of carbon (Andersen, 2003), reduced vegetation productivity (Ashmore, 2005; Felzer et al., 2004) and altered ecosystem dynamics (Agathokleous et al., 2020; Ryalls et al., 2022).

The carbon sequestration of European forest ecosystems may be significantly hindered by O_3 exposure, although modelling studies predict the extent of primary production loss to O_3 varies spatially (Proietti et al., 2016). In a *meta*-analysis of the impact of O_3 on tree growth, Wittig et al showed that the root-to-shoot ratio was significantly reduced by elevated O_3 across a range of species (Wittig et al., 2007). O_3 sensitivity varies widely across tree species (Bergmann et al., 2017), associated with differences in uptake and leaf-area-index (Feng et al., 2018) and by detoxification capacity (Li et al., 2016). O_3 exposure may lead to changes in community composition and diversity in forests (Agathokleous et al., 2020). Plant-soil-microbe interactions in forests are affected by O_3 exposure and resulting changes to leaf litter, which impacts nutrient cycling (Agathokleous et al., 2020). O_3 exposure also alters the abundance and community composition of insects in forests (Hillstrom and Lindroth, 2008), particularly beneficial invertebrates (Ryalls et al., 2024). O_3 therefore has a range of important effects on forest health and productivity.

Article 9 of the European National Emission Ceilings Directive

* Corresponding author.
E-mail address: anna.jones@biology.ox.ac.uk (A. Lee Jones).

https://doi.org/10.1016/j.ecolind.2025.113263
Received 13 November 2024; Received in revised form 23 January 2025; Accepted 17 February 2025
Available online 22 February 2025

specifies the negative impacts of air pollutants including ozone on natural and semi-natural vegetation should be monitored "…through a cost-effective and risk-based approach, based on a network of monitoring sites…" (DIRECTIVE (EU) 2016/2284 OF THE EUROPEAN PARLIAMENT AND OF THE COUNCIL on the reduction of national emissions of certain atmospheric pollutants, amending Directive 2003/35/EC and repealing Directive 2001/81/EC, 2016). Monitoring of the impacts of air pollution based upon this directive continues to apply under UK law (The National Emission Ceilings Regulations 2018, 2018). O_3 induced leaf damage can be identified in vegetation by visible foliar injury such as stippling, chlorosis and necrosis (Brace et al., 1999; Sicard et al., 2010; Treshow, 1970). Currently, the Convention on Long-range Transboundary Air Pollution (CLRTAP) and its International Co-operative Programme on Assessment and Monitoring of Air Pollution Effects on Forests (ICP Forests) recommends the assessment by visible foliar ozone injury and crown defoliation (Schaub et al., 2016). Manual leaf inspection is currently the only widescale indicator of O_3 impact on vegetation (Ferretti et al., 2024; Schaub et al., 2016). Visible foliar ozone injury is associated with decreased photosynthetic activity in sensitive species, but there is uncertainty in the suitability of visible symptoms to predict forest growth reduction (Marzuoli et al., 2019). Manual leaf inspection is inherently limited in coverage, accuracy and speed (Bussotti et al., 2003). To extend the spatial and temporal coverage of assessment of the impact of O_3 on forests, a more versatile and high throughput method is required that does not rely solely on manual leaf inspection. Assessing the extent of O_3 damage to forests is particularly important in light of ambitious reforestation targets (Abeli and Di Giulio, 2023), many of which are planned for O_3 exposed sites. Projections of carbon sequestration by afforestation, such as the European Commission's 3 Billion Tree Planting Pledge project, do not account for inhibition of productivity and growth by O_3 exposure (COMMUNICATION FROM THE COMMISSION TO THE EUROPEAN PARLIAMENT, THE COUNCIL, THE EUROPEAN ECONOMIC AND SOCIAL COMMITTEE AND THE COMMITTEE OF THE REGIONS New EU Forest Strategy for 2030: The 3 Billion Tree Planting Pledge For 2030, 2021). A comprehensive assessment of O_3 damage to forests over large spatial scales is a crucial component of both effective afforestation and monitoring the health of existing forests.

Vegetation spectroscopy uses the reflectance of light or fluorescence from vegetation to assess plant health at a range of spatial scales. Hyperspectral reflectance captures a continuous spectrum of reflectance across a range of wavelengths, versus multispectral reflectance which is confined to discrete bands of wavelengths but is more readily available. O_3 induced changes to plant health and visible foliar injury have been successfully detected using leaf reflectance in a range of species including indicator species (Meroni et al., 2008b), crops (Calzone et al., 2021; Gosselin et al., 2020; Kim et al., 2004; Marchica et al., 2019), and some trees (Diem, 2002; Gäb et al., 2006; Kefauver, 2013; Meroni et al., 2008a). In our previous study we characterised O_3 induced changes in the hyperspectral reflectance of a range of broadleaf saplings during one growth season of controlled O_3 exposure (Lee Jones et al., 2024). Hyperspectral leaf reflectance was able to differentiate between O_3 treatments and revealed a multivariate signal of O_3 damage comprised of changes in the green reflectance peak, red-edge, water absorption bands, and short wavelength infrared region. To our knowledge, no investigations have examined O_3 induced changes in the leaf reflectance of mature deciduous trees.

Pedunculate oak (*Quercus robur*) is the second most abundant broadleaf species in the UK (accounting for 16 % of broadleaved woodland), is the most common principle species, and is the largest broadleaf contributor to the UK's standing stock of timber (Forestry Statistics 2023*: Chapter 1 – Woodland Area & Planting*, 2023). Pedunculate oak also occur widely across the temperate biome and their range extends from Europe to Iran. Pedunculate oak attracts up to 2,300 associated species, of which 300 are obligate oak species (Mitchell et al., 2019). In an examination of 69 European tree species under projected climate conditions, Pedunculate oak (alongside *Fagus sylvatica* and *Quercus petraea*) was one of the only species to have high future potential to contribute to timber production, carbon uptake and habitat value (Wessely et al., 2024). Additionally Pedunculate oak is highly valued by forest managers as an iconic cultural species as well as for its timber (O'Brien et al., 2024). Pedunculate oak is therefore an important species in temperate regions and predicted to be a crucial species in the future of temperate broadleaf forests.

The effect of O_3 exposure on Pedunculate oak has been investigated under experimental conditions using seedlings and sapling trees (Cotrozzi, 2021). O_3 exposure increased photoinhibition of photosynthesis in Pedunculate oak saplings (Farage, 1996), and reduced assimilation (Calatayud et al., 2011). O_3 exposure decreased chlorophyll content in Pedunculate oak (Bussotti et al., 2007), but increased total carotenoid content and flavonoids (Pellegrini et al., 2019). O_3 exposure of Pedunculate oak saplings reduced overall biomass (Hayes et al., 2015; Moura et al., 2022), and reduced root biomass compared to shoots (Marzuoli et al., 2016). Pedunculate oak is more sensitive to O_3 than other species of oak (Moura et al., 2022; Pellegrini et al., 2019). To date, no studies have studied the effects of elevated O_3 on mature Pedunculate oak (Cotrozzi, 2021).

Tropospheric O_3 has a significant effect on the health and productivity of forests but widescale assessment of the impact of O_3 is limited by current monitoring methods. The objectives of this study were to investigate the difference in hyperspectral leaf reflectance between a low O_3 and high O_3 site, and to compare O_3 induced changes in leaf reflectance of mature trees under natural conditions to the spectral signature of O_3 damage we had experimentally elucidated in our previous study (Lee Jones et al., 2024). This study represents a crucial step in developing a high-throughput and scalable method for O_3 damage detection in broadleaf trees, by trialling hyperspectral detection in mature pedunculate oak trees in natural settings.

2. Methods

2.1. Study sites

Our study sites were two UK broadleaf woodlands with similar land use history and climate but differing predicted O_3 profiles.

Wytham Woods (UK, 51° 46′ N, 1° 20′ W) is a 400 ha research woodland owned by the University of Oxford. We accessed the canopy using the 13 m canopy walkway located in secondary woodland (Morecroft et al., 2008) within the Smithosonian Institution ForestGEO plot established in 2008 (Butt et al., 2009). The dominant soil of the plot is a well-drained Lithomorphic clay soil of Sherbourne series, above the Coral Rag limestone (Butt et al., 2009; Taylor et al., 2011). This area of Wytham is known to have been woodland since at least the 18th Century, and probably much longer (Grayson and Jones, 1956). This region of the woods is dominated by sycamore maple (*Acer psuedoplatanus*) and pedunculate oak (*Quercus robur*), as well as small numbers of common beech (*Fagus sylvatica*) (Butt et al., 2009). Ring counts of fallen trees and anecdotal evidence suggest pedunculate oak at this site are between 150–200 years old (Morecroft and Roberts, 1999). From the canopy walkway, 17 oak branches were accessible for measurements originating from four mature trees. Oak leaves emerged in early May in 2023. The long-term average rainfall of Wytham Woods is 717 mm, and average temperature 10 °C (1993–2007) (Taylor et al., 2011). Air temperature was recorded hourly from the Flux tower located close to our monitoring plot. Daily rainfall was taken from the Radcliffe Meteorological Observatory in Central Oxford due to technical issues in the Wytham Woods rainfall monitoring equipment.

Birmingham Institute for Forest Research Free-Air CO_2 Enrichment facility ('BIFoR FACE', UK, 52° 47′ N, 2° 18′ W) is a 21 ha broadleaf woodland. It is semi-natural with over 200 years continuous cover, dominated by 180 year old pedunculate oak (Hart et al., 2020). The woodland also features sycamore maple, hazel (*Corylus avellana)*,

common hawthorn (*Cretaegus monogyna*) and ash (*Fraxinus excelsior*). The dominant soil is Dystric Cambisol with sandy clay texture, and the underlying geology is Helsby Sandstone (Norby et al., 2024). BIFoR FACE has 30 m diameter experimental arrays, three of which are dosed with elevated CO_2, and three of which are controls dosed with ambient air (Hart et al., 2020). Our measurements were taken in two of the control arrays. In each control array we sampled two mature oak trees which were accessible at the canopy level, totalling four trees. Oak leaves emerged in early May in 2023. The long-term annual rainfall average is 690 mm, and average annual temperature is 9 °C (Norby et al., 2016). The mean hourly rainfall recorded by 4 rain gauges at the bottom of the BIFoR FACE meteorological towers (TR-525 M, Texas Electronics, Dallas, Texas) was totalled per day of measurement. Daily mean air temperature was averaged across 4 sensors mounted on the BIFoR FACE meteorological towers (HMP155RH, Vaisala, Helsinki, Finland).

The average accumulated O_3 exposure over the threshold of 40 ppb (AOT40) from May to July for the closest four 1 km cells in Defra's 2022 Pollution Climate Mapping Model were calculated for each site (UK AIR, Department for Environment Food & Rural Affairs (DEFRA), 2023). The average modelled background O_3 AOT40 for the BIFoR site was 4341.75 μg m^{-3} h (for O_3 1 ppb = 1.96 μg m^{-3}). This is below the UK AOT40 objective for the protection of vegetation from O_3 damage (<6000 μg m^{-3} h) (The Air Quality Limit Values Regulations 2003, n.d.). The average modelled background O_3 AOT40 for the Wytham site is 6045.5 μg m^{-3} h, this exceeds the protective threshold. Wytham Woods was designated as an O_3 polluted site based on this data, and BIFoR FACE ambient arrays designated as a lower O_3 site.

2.2. O_3 monitoring

The O_3 concentrations of both sites were monitored using Palmes-type O_3 diffusion tubes (Gradko International) between June and October 2023. Diffusion tubes were deployed at canopy level in two locations on the canopy walkway at Wytham woods and at canopy level in the two ambient arrays at BIFoR FACE. Diffusion tubes consist of a fluorinated ethylene polymer tube fitted with an absorbent cap and porosity filter to prevent ingress of particulate nitrate. Diffusion tubes were exposed on site for 2–4 weeks and then analysed by Gradko International via ion chromatography, yielding an average O_3 concentration for the exposure period. The measurement uncertainty of this analysis was quoted as ±10 % and exposure periods are given in Supplementary Material Table 1.

2.3. Leaf reflectance sampling

We measured reflectance spectra of adaxial leaf surfaces in the canopy of each site approximately every two weeks (see sampling dates in Supplementary Material, Table 1). Reflectance spectra were taken in the range 350–2500 nm with a HR-1024i spectrometer with a leaf clip and an active light source (Spectra Vista Corp, USA). The HR-1024i spectrometer is comprised of three dispersion grating spectrometers with overlapping wavelength ranges:

Very Near Infrared (VNIR), 1.5 nm sampling interval, 350–1000 nm range; Short Wavelength Infrared 1 (SWIR1), 3.8 nm sampling interval, 1000–1890 nm range; SWIR2, 2.5 nm sampling interval, 1890–2500 nm range.

The spectrometer was referenced using the incorporated leaf clip reflective standard every five minutes during measurements. Dark signal baseline correction is applied by the HR-1024i automatically, a dark spectrum is taken before each reflectance measurement. In Wytham Woods, five leaves per accessible branch were sampled per session, totalling 85 leaves from four trees. At BIFoR FACE twenty leaves were sampled from each accessible tree per measurement session, totalling 80 leaves from four trees. All leaves sampled were full developed mature leaves, without visible herbivory or mildew from the sun exposed canopy.

Table 1
Formula of common vegetation indices used to measure plant health which were tested for sensitivity to ozone damage.

Vegetation index	Equation	Reference
Normalised Difference Vegetation Index	$NDVI = \frac{\rho 800 - \rho 670}{\rho 800 + \rho 670}$	(Rouse et al., 1974)
Modified Chlorophyll Absorption Ratio Index	$MCARI = [(\rho 700 - \rho 670) - 0.2*(\rho 700 - \rho 550)]*\left(\frac{\rho 700}{\rho 670}\right)$	(Daughtry et al., 2000)
Red Edge normalised Difference Vegetation Index	$RENDVI = \frac{\rho 750 - \rho 705}{\rho 750 + \rho 705}$	(Merzlyak et al., 1999) (Sims and Gamon, 2002)
Photochemical Reflectance Index	$PRI = \frac{\rho 570 - \rho 530}{\rho 570 + \rho 530}$	(Gamon et al., 1997) (Peñuelas et al., 1995)
Plant Senescence Reflectance Index	$PSRI = \frac{\rho 680 - \rho 500}{\rho 750}$	(Merzlyak et al., 1999)
Sapling Ozone Damage Index	$OzDI = \frac{\rho 2204 - \rho 2248}{\rho 2204 + \rho 2248}$	(Lee Jones et al., 2024)

2.4. Hyperspectral processing

Leaf reflectance spectra were imported and processed as a spectral dataset in Python 3 using the SpecDAL package (Lee, 2017). The overlapping regions of the three component spectrometers in the HR-1024i were stitched. Reflectance measurements were interpolated to correspond to 1.0 nm interval wavelengths. Absolute reflectance was derived from the relative reflectance by multiplying by the known reflectance of the reference panel.

2.5. Hyperspectral analysis

Further processing of the spectral dataset was carried out in R using the 'Hyperspec' package (Beleites and Sergo, 2017). We explored the hyperspectral dataset by principal component analysis (PCA). Hyperspectral data contains many correlated variables (the wavelengths at which reflectance was sampled). We examined the clustering of spectra by site and measured O_3 concentration when plotted against combinations of principle components.

We used Partial Least-Squares Regression (PLSR) analysis as a machine learning approach to examine the relationship between hyperspectral reflectance as the predictor and O_3 concentration as the response variable. PLSR uses the least squares method to fit a linear model using partial least squares components as predictors and prevents overfitting when predictor variables are highly correlated, as is the case in hyperspectral data. PLSR was performed in R using the PLS package (Mevik and Wehrens, 2007). Per measurement session (one session per unique site/date combination) the hyperspectral data was split into test and train (30:70) and then within the test and train datasets an average spectrum was measurement session. PLSR with K-fold cross validation was applied to the train dataset and the optimal number of components was selected by minimising the root mean square error of prediction (RMSEP). This model was then applied to the test dataset and its performance in predicting O_3 concentration from hyperspectral leaf reflectance was evaluated.

To identify the spectral wavelengths most correlated to O_3 concentration, normalised difference spectral indices (NDSI) analysis was used.

NDSI is defined as:

$$NDSI(i,j) = \frac{R_i - R_j}{R_i + R_j} \quad (1)$$

where Ri is the absolute reflectance of wavelength i, and subscripts are wavelengths in nm. The average leaf reflectance spectra per measurement session (unique site/date combination) was calculated and used for NDSI analysis. All possible combinations of wavelengths (i and j) were used to calculate all NDSI. The linear relationships between the O_3 concentration and NDSIs were examined. A heat map of the absolute value of the Pearson correlation coefficient *r* between O_3 concentration and NDSI was generated. The heat maps were produced using Python 3 packages: correlation arrays were created using NumPy (Harris et al., 2020), and plotted with matplotlib (Hunter, 2007).

The NDSI with the highest correlation to O_3 concentration was compared to common vegetation indices via correlation analysis. OzDI, an infrared vegetation index corresponding to O_3 induced leaf injury in saplings derived from our previous O_3 manipulation experiment was included (Lee Jones et al., 2024). The formula of the pre-existing vegetation indices used are given in Table 2.

3. Results

3.1. O_3 and meteorological monitoring

Mean 24hr O_3 concentration over June to October 2023 was 35.54 ppb at Wytham Woods and 26.89 ppb at BIFoR FACE. The O_3 profiles of the two sites were significantly different (Mann-Whitney, $z = 0$, $p = 0.002165$). At every measurement point throughout the season Wytham Woods had higher O_3 exposure than BIFoR FACE (Fig. 1), O_3 concentrations at Wytham were also more variable. Cumulative O3 concentration is also displayed in Fig. 1B. This monitoring data, combined with Defra's AOT40 modelling for 2022 confirms that Wytham Woods is an O_3 polluted site. The maximum O_3 concentration recorded was 53.54 ppb, the average at Wytham Woods between the 7th and 27th of July 2023. The lowest O_3 concentration recorded was 24.24 ppb at BIFoR FACE between 25th July and 10th August 2023. O_3 concentration did not correlate significantly with date of measurement ($r_\tau = 31$, $p = 0.84$, Supplementary Material Fig. 2).

Throughout the measurement period (22/06/2023–06/10/2023), the average daily air temperature recorded at BIFoR FACE was 15.88 °C, and average daily rainfall was 2.14 mm. The total rainfall in the measurement period was 242.3 mm.

At Wytham Woods in the measurement period (27/06/2023–12/10/2023), the average daily air temperature was 16.29 °C. The average daily rainfall at the Radcliffe Observatory was 2.57 mm, and total rainfall in the measurement period was 277.7 mm (Burt and Burt, 2019).

3.2. Visual observations

In Wytham Woods, pinprick white dots (stippling) were observed on the adaxial leaf surface of oaks (Supplementary Material, Fig. 1), no stippling was observed at BIFoR FACE. Stippling indicates a programmed cell death response, which occurs in response to O_3 stress but may also indicate other stressors. The stippling of oak leaves at Wytham Woods avoided the veins and was more prevalent on leaves at the ends of branches, which is typical of O_3 induced injury. Herbivory and mildew on some leaf surfaces were also observed at both sites, leaf reflectance measurements were not taken from affected leaves.

Table 2
Results of Pearson correlation analysis of different vegetation indices against average O_3 concentration. *** indicates P value < 0.001.

vegetation index	Correlation	Degrees of Freedom	T Value	P Value
NDVI	0.52	10	1.92	0.0832
MCARI	0.826	10	4.63	0.000933 ***
PRI	0.0273	10	0.0864	0.933
PSRI	−0.563	10	−2.15	0.0569
Max NDSI	0.839	10	4.88	0.000639 ***
OzDI	−0.301	10	−0.997	0.342

3.3. Hyperspectral leaf reflectance

The average hyperspectral reflectance of oak leaves from Wytham Woods and BIFoR FACE exhibited a pattern of typical foliar reflectance but differed in intensity at key regions of the spectrum (Fig. 2). The intensity of the green reflectance peak (~540 nm) was greater in leaves from Wytham Woods, as was the triple reflectance peak in the Near Infrared (750 – 1300 nm). At the water absorption bands (1400 nm and 1900 nm), leaves from BIFoR FACE had shallower reflectance troughs than leaves from Wytham Woods. Leaves from BIFoR FACE also had increased reflectance intensity in the short wavelength infrared peak at 2200 nm compared to leaves from Wytham Woods.

3.4. Principal component analysis

The first four principal components of the hyperspectral dataset of leaf reflectance were cumulatively able to explain 98.8 % of the variance in the dataset (PC1 84.78 %, PC2 11.44 %, PC3 1.99 %, PC4 0.6 %). The Scree Plot of principle components can be found in the Supplementary Material, Fig. 3. The first principal component (PC1) was loaded most heavily by wavelengths in the near-infrared (NIR) and infrared (Fig. 3A). PC1 captures the generic profile of leaf reflectance spectra, and so summarises differences in overall reflectance intensity. The second principal component (PC2) was negatively correlated with wavelengths in the Red-Edge and NIR, and positively correlated with wavelengths in the infrared (Fig. 3A). The third principal component (PC3) was strongly loaded by wavelengths in the green peak and red edge, commonly used to assess chlorophyll content (Fig. 3A). Principle component four (PC4) was loaded heavily by the lower boundary of wavelengths measured by the spectrometer (~350 nm), and negatively correlated to the Near infrared (Fig. 3A).

Fig. 3B-D shows the clustering of leaf reflectance spectra coloured by measurement site against combinations of the first three principal components. There is separation of leaf reflectance spectra from BIFoR FACE versus Wytham Woods in all three combinations of PCs, but components two and three achieve the clearest distinction between sites (Fig. 3C). The reflectance spectra of leaves at BIFoR FACE versus Wytham Woods can be discriminated by principal components, and therefore differ. The difference in reflectance spectra between the two sites correlates with cumulative O_3 concentration (Fig. 3E), and average O3 concentration (Supplementary Material Fig. 4) but not with date of measurement (Supplementary Material Fig. 5). Leaf reflectance clustered most clearly by average and cumulative O_3 concentration when plotted against the first two principal components (Fig. 3E).

The reflectance spectra of leaves from BIFoR FACE versus Wytham Woods are therefore distinct and the differences between the sites correlate with both average and cumulative O_3 concentration. The variation in reflectance spectra is best characterised by the overall intensity of leaf reflectance (PC1) combined with the intensity of the green peak (PC3), Red-Edge (PC1, 2 and 3) and infrared reflectance peaks.

3.5. Partial least squares regression analysis

We selected a two component PLSR model for our analysis, based on minimisation of RMSEP in the train dataset (Fig. 4A). These two latent variables explained 89 % of variance in the reflectance data (component 1: 37 %, component 2: 52 %) and 56 % of variance in O_3 concentration. Component 1 was strongly positively loaded by reflectance in the green peak, NIR, and to a weaker extent negatively loaded in the SWIR

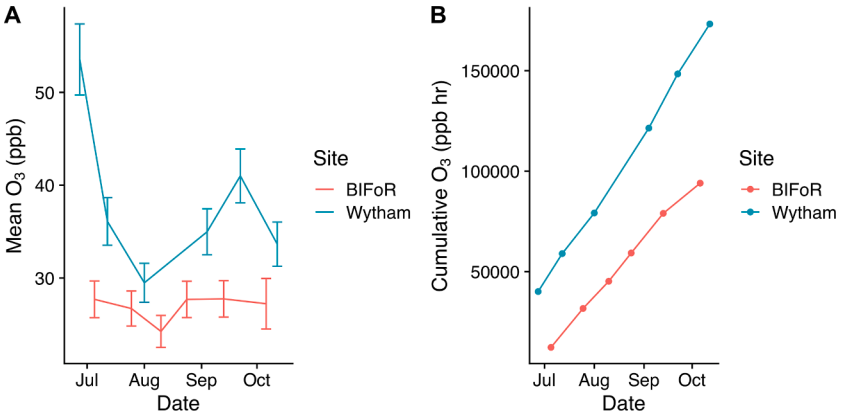

Fig. 1. Time series of O_3 concentrations at Wytham Woods (blue) and BIFoR FACE facility (red) from July to October 2023. A: Mean hourly O3 concentrations in ppb calculated from the preceding measurement period, error bars represent the mean measurement uncertainty at each time point. B: Cumulative O3 dosage in ppb hour from 26th June 2023 at BIFoR FACE facility, and from the 27th June 2023 at Wytham woods.

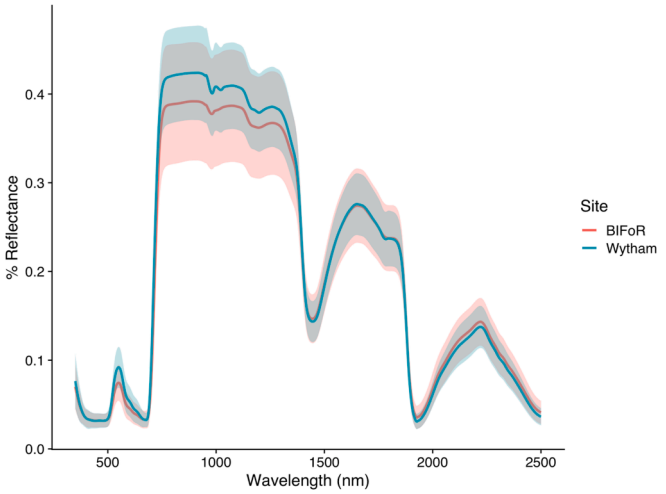

Fig. 2. Average hyperspectral leaf reflectance per site displayed as a solid line (BIFoR FACE facility in red, Wytham Woods in blue), with ± standard deviation surrounding the mean in shading (BIFoR FACE facility in light red, Wytham Woods in light blue).

(Fig. 4B). Component 2 also featured the Red Edge and was strongly negatively loaded in SWIR of the spectra (Fig. 4B). When the PLSR model with 2 components was used to predict O_3 values from the test spectral dataset, it achieved RMSE of 5.33, R^2 0.588 and MAE 4.34. Fig. 4C shows the capacity of the model to predict O_3 concentrations (as an indicator of the stress due to ozone) experienced by the leaves based on their reflectance spectra alone, which are a close match to observed O_3 concentrations. The accuracy of prediction of O_3 concentration decreases at higher concentrations, as shown by the confidence boundaries in Fig. 4C. The coefficient of the line of best fit is 0.63, indicating the model somewhat underestimates O_3 concentration on average.

3.6. Normalised difference spectral indices analysis

The correlation of all possible normalised difference indices to O_3 concentration is displayed as a heatmap in Fig. 5. NDSIs which combined one wavelength Red Edge (740–760 nm) and a wavelength above 760 nm were highly correlated to O_3 concentration (Fig. 5). Combinations of wavelengths between 500–750 nm were also highly correlated to O_3 concentration, these wavelengths characterise the shape of the green reflectance peak and Red Edge. Many other wavelength combinations were strongly correlated to O_3 concentration, including wavelengths from 1900-2000 nm and combinations of ~ 1500 to 2000 + nm. The combination of wavelengths most highly correlated with O_3 concentration were 515 nm and 647 nm, which characterise the width and intensity of the green reflectance peak. This index will be referred to as "Max NDSI".

3.7. Vegetation indices

Some pre-existing vegetation indices showed strong relationships with average O_3 concentration (Fig. 6) and weaker relationships with cumulative O_3 concentration (Supplementary Material Fig. 6 and Table 1). Modified Chlorophyll Absorption Ratio Index (MCARI) was significantly correlated with average O_3 (Table 3). MCARI combines reflectance intensities at 700, 670 and 550 nm (Table 2), and is inversely related to chlorophyll content. MCARI showed a strong positive correlation with O_3 concentration ($r(10) = 0.826$, $p < 0.001$). MCARI was not correlated with date of measurement ($r(12) = 0.161$, $p = 0.96$), but was significantly higher at Wytham Woods than BIFoR FACE ($t(13) = -6.42$, $p < 0.001$).

Normalised Difference Vegetation Index (NDVI) was weakly positively correlated to average O_3 concentration (Fig. 6A), but this relationship was not significant (Table 3). NDVI was significantly positively correlated with cumulative O_3 concentration (Supplementary Material Fig. 6A, $r(10) = 0.690$, $p = 0.0131$). PSRI was negatively correlated with average O_3 concentration (Fig. 6D), but again this relationship was not significant (Table 3). There was no clear relationship between OzDI and average O_3 concentration (Fig. 6f). OzDI was significantly positively correlated with cumulative O_3 concentration (Supplementary Material Fig. 6F, $r(10) = 0.661$, $p = 0.0193$), however there was a clear site specific difference in the correlation of this relationship.

The Max NDSI calculated from this hyperspectral dataset as described above, was positively correlated with average O_3 concentration (Fig. 6E). The strong positive correlation between Max NDSI and average O_3 concentration was statistically significant ($r(10) = 0.839$, $p < 0.001$).

4. Discussion

Our O_3 monitoring in Wytham Woods demonstrates the site is exposed to damaging levels of O_3, as predicted by the Defra's Pollution Climate Mapping Model. The meteorological conditions of the two sites were similar in terms of rainfall and temperature, however other factors such as light availability, humidity, and soil nutrients may also affect leaf reflectance (Baltzer and Thomas, 2005). The scope of this study did not include the measurement of additional meteorological factors which may differ between the two woodlands, meaning hyperspectral features

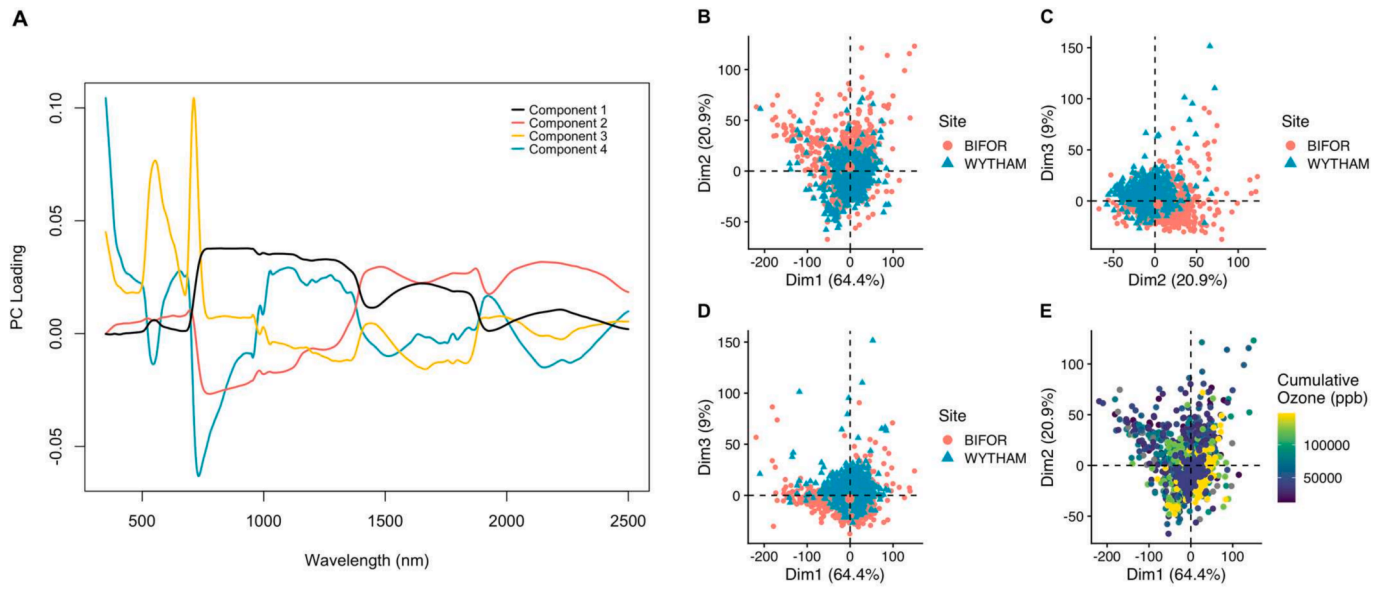

Fig. 3. Principal component analysis of hyperspectral leaf reflectance from the two study sites (BIFoR in red, Wytham in blue). A: Loadings of the first four principal component (PC) across the spectra of wavelengths measured. B: Leaf reflectance coloured by site against PC1 and PC2. C: leaf reflectance coloured by site against PC2 and PC3. D: Leaf reflectance coloured by site against PC1 and PC3. E: Leaf reflectance coloured by cumulative ozone concentration in ppb against PC1 and PC2.

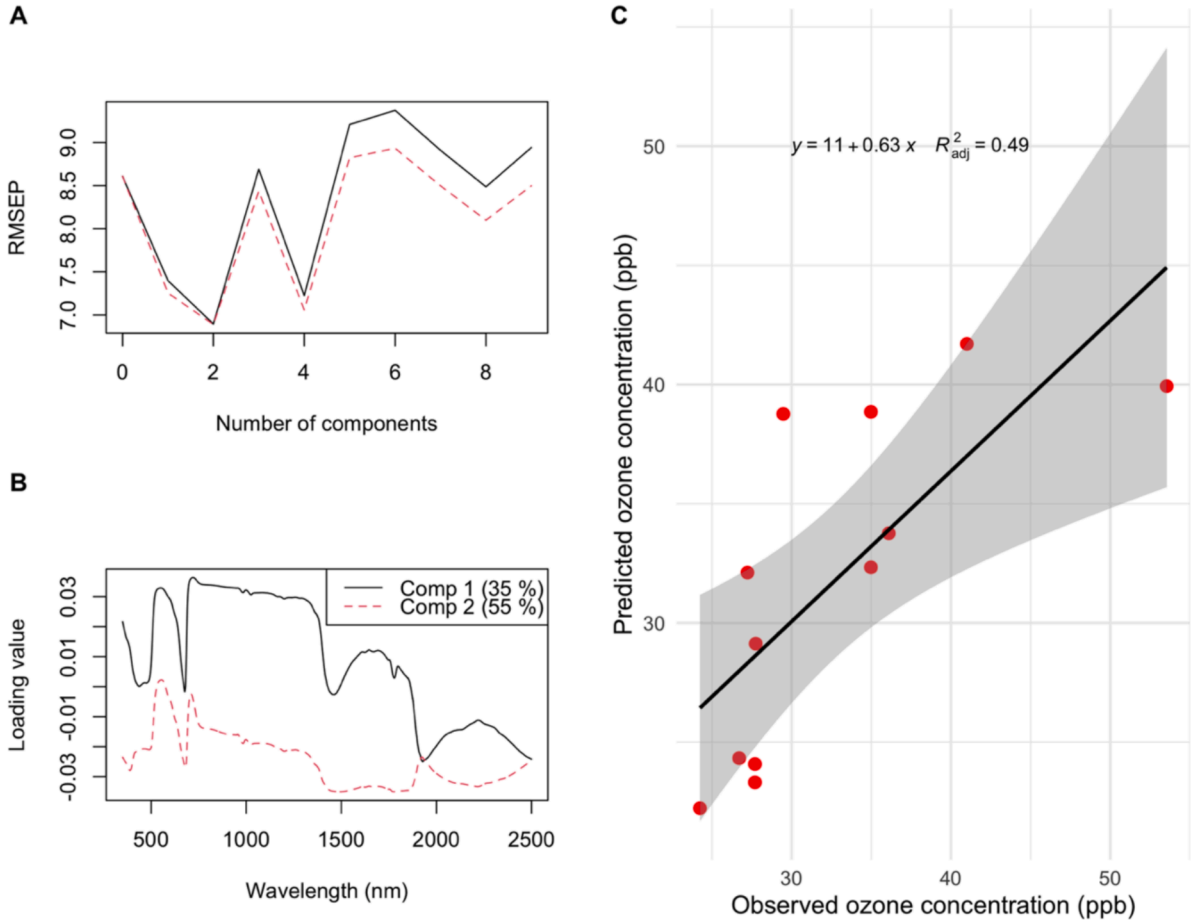

Fig. 4. Partial least squares regression (PLSR) model validation and predictions of O_3 concentration from hyperspectral leaf reflectance. A: PLSR root mean square error prediction (RMSEP) versus number of model components. B: Loadings of the first two PLS components across the range of reflectance wavelengths measured. C: Ozone concentrations predicted by the model versus observed ozone concentrations, based on hyperspectral leaf reflectance of the test dataset.

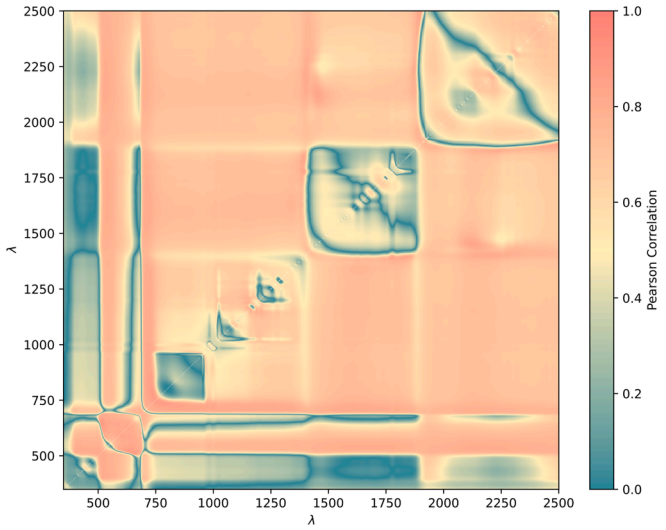

Fig. 5. Heatmap of the Pearson correlation of the normalised difference of wavelength combinations to O_3 concentration. Lambda, λ, represents wavelength in nm.

which correlated with ozone over time and without site specific differences are more robust such as the PLSR analysis. The canopy in Wytham Woods was significantly more O_3 exposed than BIFoR FACE, and the differences in leaf reflectance between the two sites indicate foliar changes induced by O_3 damage.

The cumulative exposure of vegetation to O_3 determines the magnitude of damage (Bastrup-Birk et al., 1997). AOT40 has been adopted widely as a metric of "accumulate ozone over threshold 40 ppb" intended to capture vegetation damaging levels of ozone exposure for compliance monitoring. However, there is developing scientific consensus that a stomatal flux-based approach gives a more accurate assessment of the risk of O_3 damage to vegetation (Mills et al., 2011; Proietti et al., 2021; Sicard et al., 2016). Stomatal O_3 flux is affected by atmospheric and stomatal conductivity (Guderian, 1985). There are a range of species specific or vegetation type POD_y flux models which calculate the cumulative exceedance of critical levels of stomatal O_3 flux, based on O_3 concentration, temperature, humidity, light and soil moisture (Mills et al., 2017). Hourly monitoring of these parameters was beyond the scope of this study, and so we use simple ozone concentration and cumulative ozone concentration as a proxy for ozone dosage which has obvious limitations in terms of understanding the dose of ozone received.

The O_3 induced change in leaf reflectance we identified is multivariate, key regions of the spectra include the green reflectance peak, red edge, and NIR. The hyperspectral reflectance profile of oak leaves at Wytham Woods, the high O_3 site, was increased in the height and width of the green reflectance peak (500—570 nm) and the Near Infrared triple peak (750–1300 nm). In the water absorption peaks (1400 nm and 1900 nm), and infrared peak at 2200 nm the leaf reflectance of the high

Table 3
Results of Pearson correlation analysis of different vegetation indices against average O_3 concentration.

Vegetation index	Correlation	Degrees of freedom	T value	P value
NDVI	0.52	10	1.92	0.0832
MCARI	0.826	10	4.63	0.000933***
PRI	0.0273	10	0.0864	0.933
PSRI	−0.563	10	−2.15	0.0569
Max NDSI	0.839	10	4.88	0.000639***
OzDI	−0.301	10	−0.997	0.342

***indicates P value < 0.001.

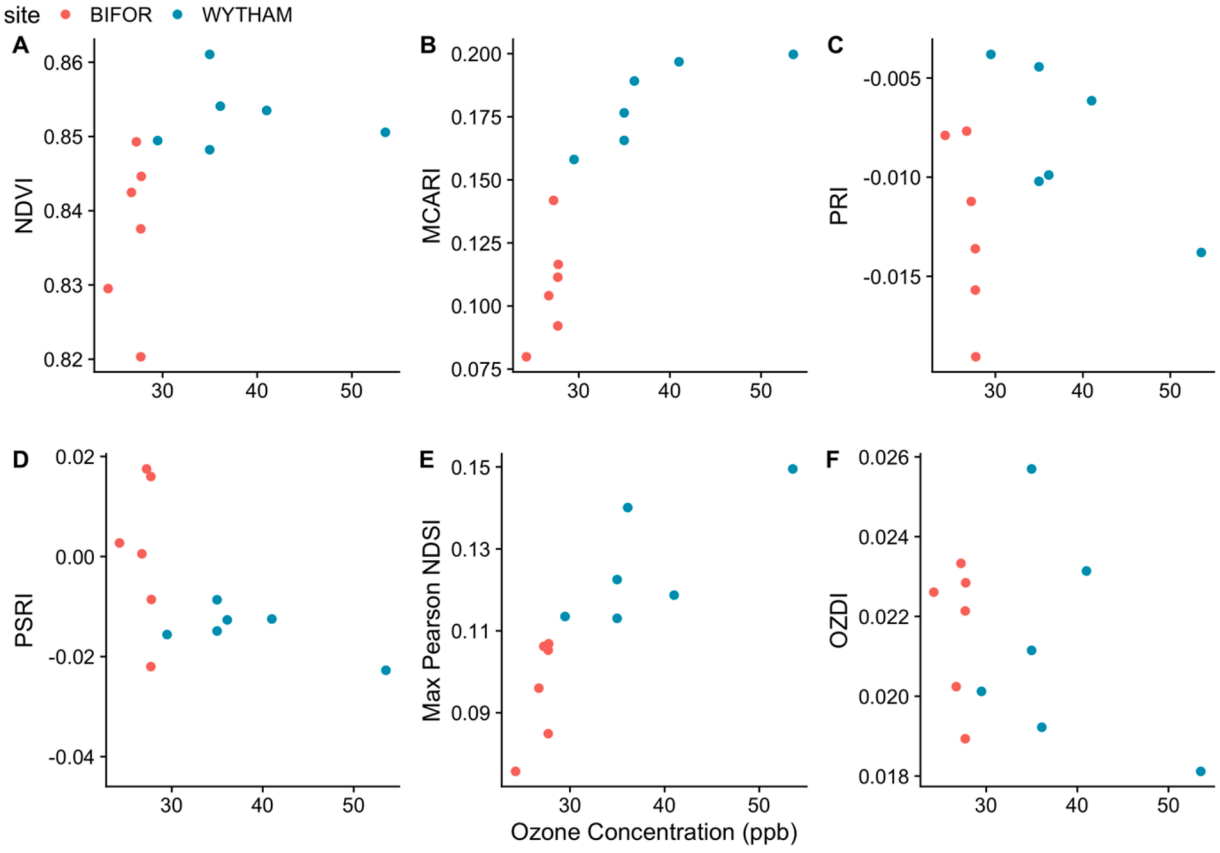

Fig. 6. Vegetation indices plotted against ozone concentration, coloured by site of measurement (BIFoR in red, Wytham Woods in blue).

and low O_3 was more similar, although slightly reduced under high O_3. Unsupervised variable reduction (PCA) and supervised variable reduction (PLSR) both highlighted the green reflectance peak and near infrared triple peak as key regions for summarising the variability in hyperspectral reflectance profiles. The high spectral resolution and wavelength range of our measurements allow a more detailed understanding of the spectral shifts underpinning changes in vegetation indices and the multivariate differences in leaf reflectance between a low and high O_3 site.

The indices most strongly related to average O_3 exposure independent of site (max NDSI and MCARI) characterise the intensity and width of the green reflectance peak (500–650 nm). Several early experimental studies found changes in this region associated with O_3 damage in other species (Meroni et al., 2009; Ustin and Curtiss, 1990). PRI characterises the top of the green reflectance peak at 550 nm but did not respond significantly to O_3 exposure in neither our field or experimental study, whereas max NDSI and MCARI characterise the broader green reflectance peak by inclusion of a wavelength at 640–670 nm. The green reflectance peak is influenced by chlorophyll, carotene and anthocyanin pigment concentrations in combination (Sims and Gamon, 2002). Chlorophyll content decreases during ozone stress (Knudson et al., 1977), whereas anthocyanins are an anti-oxidant upregulated to in response to the oxidative stress caused by high ozone (Chalker-Scott, 1999). MCARI was developed to estimate chlorophyll *A* concentration (Daughtry et al., 2000), but is also influenced by xanthophyll and carotene concentration (Taylor-Zavala et al., 2021). NDVI characterises the red edge and is dominated by chlorophyll *A* concentration but did not respond to O_3 exposure. In O_3 exposed oak saplings, a significant increase in total carotenoids (including carotene and xanthophylls) has been observed experimentally (Pellegrini et al., 2019). Together these results indicate the broader green reflectance peak is a key component of the signal of O_3 damage in leaf reflectance, likely underpinned by changes in the relative concentration of chlorophyll, carotene, and xanthophyll pigments.

The effects of O_3 on oak species was reviewed by Cotrozzi in a *meta*-analysis which concluded that although oak species are broadly resistant to large changes in biomass under elevated O_3 damage, they undergo significant physiological impairment (Cotrozzi, 2021). O_3 exposure reduced the maximum rate of carboxylation, electron transport rate, conductance parameters and stomatal responsivity in 2 year-old *Quercus robur* (Hoshika et al., 2022). Phenols play a key role in the antioxidant response of oak species (Cotrozzi, 2021). These physiological effects may relate to the changes we have observed in the green peak leaf reflectance peak, but further studies are needed to identify the precise leaf level changes underpinning changes in leaf reflectance in response to O_3. A further limitation of current knowledge of the effects of O_3 on forests is a lack of studies on mature trees, which we sought to address although this limited our study to a 'natural experiment' with many uncontrolled variables in comparison to the many O_3 manipulation studies on young trees.

Leaf reflectance is affected by many factors, besides O_3 damage, such as drought (Sapes et al., 2024), disease (Fallon et al., 2020), and leaf traits (Yang et al., 2016). However, the changes in leaf reflectance we found corresponded strongly to O_3 concentration changes within as well as between the two sites. Our machine learning model of hyperspectral reflectance was able to accurately predict O_3 exposure from reflectance data, independent of study site. Furthermore, we also demonstrated that MCARI and the Max NDSI responded linearly to O_3 concentrations across both sites. Date of measurement did not have a significant relationship with O_3 concentration, and did not significantly affect MCARI. In our previous experimental study, the MCARI of oak saplings also changed significantly under different O_3 exposure regimes (Lee Jones et al., 2024). The principal components of the hyperspectral dataset show similarities between the present field study and our previous controlled experiment, suggesting broadly similar regions of variation in the leaf reflectance spectra. The width of the green reflectance peak (characterised by MCARI and Max NDSI) was important in differentiating between O_3 treatments in our previous controlled experiment, as well as in the present field study.

Conversely, the short wavelength infrared region (SWIR) which varied strongly with foliar O_3 damage in our previous controlled experiment did not show a relationship with O_3 concentration in the present field study. There are several possible reasons for this: maximum O_3 concentrations measured in the field were lower than the highest O_3 treatment in our previous experiment and so changes in the SWIR may only be triggered at higher O_3 concentrations. Some studies have also found that juvenile trees are more sensitive to O_3 stress than mature tress due to higher stomatal uptake and therefore dosage of O_3 (Nunn et al., 2005). Alternatively, the SWIR region may be affected by O_3 in saplings but not in mature trees. Stress responses are known to differ between saplings and mature trees for example in response to drought in *Quercus rubra* (Cavender-Bares and Bazzaz, 2000), other studies of *Quercus* and deciduous species have found age-related differences in leaf traits and gas exchange patterns (Mediavilla and Escudero, 2003; Thomas and Winner, 2002). The SWIR region of leaf reflectance is associated with foliar cellulose, starch, and sugar content, as well as water content (Cheng et al., 2011; Curran, 1989) and so may be affected differently by O_3 stress in saplings versus mature trees. Conversely, some studies have shown similar responses to O_3 stress in saplings and mature trees (Braun et al., 2014). These two explanations for the difference in SWIR response between our two studies (lower O_3 exposure/uptake and differences in ontogeny) are not mutually exclusive.

We have demonstrated using a machine learning approach that O_3 exposure in mature trees can be detected from hyperspectral leaf reflectance (PLSR analysis), which could be used to indicate locally damaging O_3 concentrations. Tropospheric O_3 monitoring is sparse in coverage, and focusses on urban versus suburban sites in the UK (Finch and Palmer, 2020). The O_3 exposure of most forests is unknown, and monitoring requires expensive automated gas analysers or regular lab analysis of diffusion tubes. Leaf reflectance therefore represents an exciting new method of identifying damage inducing O_3 concentrations in forests, confirmed by air pollution models. We took leaf level reflectance measurements directly from the canopy, but scaling this method up to remote measurements taken via unmanned aerial vehicles (UAV, or drones) would allow widespread assessment of O_3 induced damage in forests.

Although this study focussed on oak, our previous O_3 exposure experiment showed oak reflectance in saplings responded similarly to other broadleaf species (beech, birch, alder and crab apple). MCARI differed significantly with O_3 treatment across beech, birch, crab apple as well as oak in our experimental study. Meroni et al reported similar changes in the green peak and red edge in *Populus nigra* (Meroni et al., 2009). We hypothesize hyperspectral detection of O_3 damage using analysis of the green peak and red edge in mature trees could be expanded beyond oak to other deciduous species. The canopies of natural or semi natural deciduous forests are often a mixture of different species, and so expanding detection of O_3 damage to a deciduous species mix will be important for developing a remote sensing method of O_3 damage detection.

The spectral method of O_3 damage detection we have tested is more scalable and consistent than manual inspection of foliar damage. Hyperspectral measurements are not subjectively influence by the assessor, unlike manual inspection methods. Standardisation training for human O_3 damage assessors can improve the subjectivity of their measurements, but differences remain and training takes significant resources (Bussotti et al., 2003). Hyperspectral measurements on the other hand are objective, standardised by referencing, and can be taken by non-experts. Hyperspectral measurements can also be taken remotely via UAV, aircraft and satellite although scaling spectral intensity across spatial scales can be challenging (Fawcett et al., 2020). Vegetation indices are directly scalable however because by taking the ratio of intensity at different wavelengths, they are not dependant on absolute

intensity of reflectance. MCARI has a strong relationship with O_3 exposure and can be calculated from multispectral satellites with global coverage over several decades such as Sentinel 2 and Landsat 8. Standard multispectral satellite bands could not be used to calculate Max NDSI but hyperspectral satellite products such as EnMAP could be used on a landscape scale to assess O_3 damage to vegetation. This study demonstrates the potential for specific changes in leaf reflectance to be used to monitor O_3 damage on larger spatial scales in a new application of remote sensing.

5. Conclusions

Our study has shown a clear signal of O_3 damage can be detected from hyperspectral leaf reflectance in adult oak trees under a range of naturally occurring O_3 concentrations. Hyperspectral leaf reflectance can be used to accurately predict O_3 exposure, which could be scaled up for forest level assessments of damage inducing O_3 exposure. O_3 induced changes in leaf reflectance can be tracked using vegetation indices such as MCARI, which could be used establish remote sensing of O_3 damage to forests. As O_3 concentrations continue to rise globally, understanding the extent of O_3 damage to forests is crucial to effectively harness the carbon sequestration potential of forests. We have demonstrated the exciting potential of spectral monitoring of O_3 damage in mature trees, which now needs to be generalised beyond oak and scaled up to a remote sensing methodology.

CRediT authorship contribution statement

Anna Lee Jones: Writing – review & editing, Writing – original draft, Visualization, Validation, Software, Project administration, Methodology, Investigation, Formal analysis, Data curation, Conceptualization. **Christian Pfrang:** Writing – review & editing, Supervision. **Felicity Hayes:** Writing – review & editing, Supervision. **Elizabeth S. Jeffers:** Writing – review & editing, Supervision, Conceptualization.

Declaration of competing interest

The authors declare that they have no known competing financial interests or personal relationships that could have appeared to influence the work reported in this paper.

Acknowledgements

This work was supported by the Natural Environment Research Council [grant number NE/S007474/1]. The SVC HR-1024i, leaf clip-reflectance probe attachment, and reflectance panels, were loaned from the National Environment Research Council Field Spectroscopy Facility (NERC FSF) under FSF internal loan number 915.1122. The authors gratefully acknowledge NERC FSF for this loan, and for the training and technical advice provided.

Fieldwork carried out at the Birmingham Institute of Forest Research FACE Facility was coordinated by Dr Kris Hart and academically supervised by Prof Christian Pfrang. The authors would like to thank Peter Miles for his enthusiasm and facilitation of canopy access at BIFoR FACE. BIFoR FACE meteorological data was collected and managed by the following contributors: Curioni G., Denny G., Downes T.M., Harper N.J., Hart K.M., Mackenzie A.R., Miles P., Ullah S., Tekinay F. The BIFoR FACE facility is a research infrastructure project supported by the JABBS Foundation and the University of Birmingham. The facility has received support for scientific studies from the Biotechnology and Biological Sciences Research Council (BBSRC), Ecological Continuity Trust (ECT), JABBS Foundation, the John Horseman Trust, the Natural Environment Research Council (NERC), National Science Foundation (NSF), the Woodland Trust and the Newton Fund.

We would also like to thank Alex Black, Yadvinder Mahli, and Curt Lambeth for facilitating canopy access in Wytham Woods and meteorological data. We thank Adam Ormondroyd for software consultation and heat map advice.

Appendix A. Supplementary data

Supplementary data to this article can be found online at https://doi.org/10.1016/j.ecolind.2025.113263.

Data availability

Data is available at https://doi.org/10.5281/zenodo.13928876, and code at https://github.com/Anna-Lee-Jones/On-Mature-Reflection-2024.git

References

Abeli, T., Di Giulio, A., 2023. Risks of massive tree planting in Europe should be considered by the EU Forestry Strategy 2030. Restor. Ecol. 31, e13834. https://doi.org/10.1111/rec.13834.

Agathokleous, E., Feng, Z., Oksanen, E., Sicard, P., Wang, Q., Saitanis, C.J., Araminiene, V., Blande, J.D., Hayes, F., Calatayud, V., Domingos, M., Veresoglou, S. D., Peñuelas, J., Wardle, D.A., Marco, A.D., Li, Z., Harmens, H., Yuan, X., Vitale, M., Paoletti, E., 2020. Ozone affects plant, insect, and soil microbial communities: a threat to terrestrial ecosystems and biodiversity. Sci. Adv. 6, eabc1176. https://doi.org/10.1126/sciadv.abc1176.

Andersen, C.P., 2003. Source–sink balance and carbon allocation below ground in plants exposed to ozone. New Phytol. 157, 213–228. https://doi.org/10.1046/j.1469-8137.2003.00674.x.

Ashmore, M.R., 2005. Assessing the future global impacts of ozone on vegetation. Plant Cell Environ. 28, 949–964. https://doi.org/10.1111/j.1365-3040.2005.01341.x.

Baltzer, J.L., Thomas, S.C., 2005. Leaf optical responses to light and soil nutrient availability in temperate deciduous trees. Am. J. Bot. 92, 214–223. https://doi.org/10.3732/ajb.92.2.214.

Bastrup-Birk, A., Brandt, J., Zlatev, Z., Uria, I., 1997. Studying cumulative ozone exposures in Europe during a 7-year period. J. Geophys. Res. Atmospheres 102, 23917–23935. https://doi.org/10.1029/97JD01966.

Beleites, C., Sergo, V. 2017. hyperSpec: a package to handle hyperspectral data sets in R.

Bergmann, E., Bender, J., Weigel, H.-J., 2017. Impact of tropospheric ozone on terrestrial biodiversity: a literature analysis to identify ozone sensitive taxa. J. Appl. Bot. Food Qual. 90, 83–105. https://doi.org/10.5073/JABFQ.2017.090.012.

Brace, S., Peterson, D.L., Bowers, Darci., 1999. A guide to ozone injury in vascular plants of the Pacific Northwest. (No. PNW-GTR-446). U.S. Department of Agriculture, Forest Service, Pacific Northwest Research Station, Portland, OR. https://doi.org/10.2737/PNW-GTR-446.

Braun, S., Schindler, C., Rihm, B., 2014. Growth losses in Swiss forests caused by ozone: epidemiological data analysis of stem increment of *Fagus sylvatica* L. and *Picea abies* Karst. Environ. Pollut. 192, 129–138. https://doi.org/10.1016/j.envpol.2014.05.016.

Burt, S., Burt, T., 2019. Oxford Weather and Climate Since 1767 (Updated to 2023 from SOGE website.). Oxford University Press.

Bussotti, F., Desotgiu, R., Cascio, C., Strasser, R.J., Gerosa, G., Marzuoli, R., 2007. Photosynthesis responses to ozone in young trees of three species with different sensitivities, in a 2-year open-top chamber experiment (Curno, Italy). Physiol. Plant. 130, 122–135. https://doi.org/10.1111/j.1399-3054.2007.00894.x.

Bussotti, F., Schaub, M., Cozzi, A., Kräuchi, N., Ferretti, M., Novak, K., Skelly, J.M. 2003. Assessment of ozone visible symptoms in the field: perspectives of quality control. Environ. Pollut., Native Plants as Bioindicators of Air Pollutants: Contributed Papers to a Symposium held in conjunction with the 34th Air Pollution Workshop 125, 81–89. https://doi.org/10.1016/S0269-7491(03)00095-2.

Butt, N., Campbell, G., Malhi, Y., Morecroft, M., Fenn, K., Thomas, M., 2009. Initial Results from Establishment of a Long-term Broadleaf Monitoring Plot at Wytham Woods, Oxford, UK.

Calatayud, V., Cerveró, J., Calvo, E., García-Breijo, F.-J., Reig-Armiñana, J., Sanz, M.J., 2011. Responses of evergreen and deciduous *Quercus* species to enhanced ozone levels. Environ. Pollut. 159, 55–63. https://doi.org/10.1016/j.envpol.2010.09.024.

Calzone, A., Cotrozzi, L., Remorini, D., Lorenzini, G., Nali, C., Pellegrini, E., 2021. Oxidative stress assessment by a spectroscopic approach in pomegranate plants under a gradient of ozone concentrations. Environ. Exp. Bot. 182, 104309. https://doi.org/10.1016/j.envexpbot.2020.104309.

Cavender-Bares, J., Bazzaz, F.A., 2000. Changes in drought response strategies with ontogeny in Quercus rubra: implications for scaling from seedlings to mature trees. Oecologia 124, 8–18. https://doi.org/10.1007/PL00008865.

Chalker-Scott, L., 1999. Environmental significance of anthocyanins in plant stress responses. Photochem. Photobiol. 70, 1–9. https://doi.org/10.1111/j.1751-1097.1999.tb01944.x.

Cheng, T., Rivard, B., Sánchez-Azofeifa, A., 2011. Spectroscopic determination of leaf water content using continuous wavelet analysis. Remote Sens. Environ. 115, 659–670. https://doi.org/10.1016/j.rse.2010.11.001.

Christiansen, A., Mickley, L.J., Liu, J., Oman, L.D., Hu, L., 2022. Multidecadal increases in global tropospheric ozone derived from ozonesonde and surface site observations:

can models reproduce ozone trends? Atmos. Chem. Phys. 22, 14751–14782. https://doi.org/10.5194/acp-22-14751-2022.
COMMUNICATION FROM THE COMMISSION TO THE EUROPEAN PARLIAMENT, THE COUNCIL, THE EUROPEAN ECONOMIC AND SOCIAL COMMITTEE AND THE COMMITTEE OF THE REGIONS New EU Forest Strategy for 2030: The 3 Billion Tree Planting Pledge For 2030, 2021. , 52021SC0651.
Cooper, O.R., Parrish, D.D., Ziemke, J., Balashov, N.V., Cupeiro, M., Galbally, I.E., Gilge, S., Horowitz, L., Jensen, N.R., Lamarque, J.-F., Naik, V., Oltmans, S.J., Schwab, J., Shindell, D.T., Thompson, A.M., Thouret, V., Wang, Y., Zbinden, R.M., 2014. Global distribution and trends of tropospheric ozone: an observation-based review. Elem. Sci. Anthr. 2, 000029. https://doi.org/10.12952/journal.elementa.000029.
Cotrozzi, L., 2021. The effects of tropospheric ozone on oaks: a global meta-analysis. Sci. Total Environ. 756, 143795. https://doi.org/10.1016/j.scitotenv.2020.143795.
Curran, P.J., 1989. Remote sensing of foliar chemistry. Remote Sens. Environ. 30, 271–278. https://doi.org/10.1016/0034-4257(89)90069-2.
Daughtry, C.S.T., Walthall, C.L., Kim, M.S., de Colstoun, E.B., McMurtrey, J.E., 2000. Estimating corn leaf chlorophyll concentration from leaf and canopy reflectance. Remote Sens. Environ. 74, 229–239. https://doi.org/10.1016/S0034-4257(00)00113-9.
Diem, J.E., 2002. Remote assessment of forest health in Southern Arizona, USA: evidence for ozone-induced foliar injury. Environ. Manage. 29, 373–384. https://doi.org/10.1007/s00267-001-0011-5.
DIRECTIVE (EU) 2016/2284 OF THE PARLIAMENT AND OF THE COUNCIL on the reduction of national emissions of certain atmospheric pollutants, amending Directive 2003/35/EC and repealing Directive 2001/81/EC, 2016.
Donzelli, G., Suarez-Varela, M.M., 2024. Tropospheric ozone: a critical review of the literature on emissions, exposure, and health effects. Atmosphere 15, 779. https://doi.org/10.3390/atmos15070779.
Fallon, B., Yang, A., Lapadat, C., Armour, I., Juzwik, J., Montgomery, R.A., Cavender-Bares, J., 2020. Spectral differentiation of oak wilt from foliar fungal disease and drought is correlated with physiological changes. Tree Physiol. 40, 377–390. https://doi.org/10.1093/treephys/tpaa005.
Farage, P.K., 1996. The effect of ozone fumigation over one season on photosynthetic processes of Quercus robur seedlings. New Phytol. 134, 279–285. https://doi.org/10.1111/j.1469-8137.1996.tb04632.x.
Fawcett, D., Panigada, C., Tagliabue, G., Boschetti, M., Celesti, M., Evdokimov, A., Biriukova, K., Colombo, R., Miglietta, F., Rascher, U., Anderson, K., 2020. Multi-scale evaluation of drone-based multispectral surface reflectance and vegetation indices in operational conditions. Remote Sens. 12, 514. https://doi.org/10.3390/rs12030514.
Felzer, B., Kicklighter, D., Melillo, J., Wang, C., Zhuang, Q., Prinn, R., 2004. Effects of ozone on net primary production and carbon sequestration in the conterminous United States using a biogeochemistry model. Tellus B Chem. Phys. Meteorol. 56, 230–248. https://doi.org/10.3402/tellusb.v56i3.16415.
Feng, Z., Büker, P., Pleijel, H., Emberson, L., Karlsson, P.E., Uddling, J., 2018. A unifying explanation for variation in ozone sensitivity among woody plants. Glob. Change Biol. 24, 78–84. https://doi.org/10.1111/gcb.13824.
Ferretti, M., Cailleret, M., Haeni, M., Trotsiuk, V., Apuhtin, V., Araminiene, V., Buriánek, V., Cecchini, S., Dalstein-Richier, L., Hůnová, I., Jakovljević, T., Kaoukis, K., Neirynck, J., Nicolas, M., Prescher, A.-K., Novotný, R., Pavlendova, H., Potočić, N., Rupel, M., Russ, A., Stakėnas, V., Verstraeten, A., Vollenweider, P., Zlindra, D., Pitar, D., Calatayud, V., Gottardini, E., Schaub, M., 2024. The fingerprint of tropospheric ozone on broadleaved forest vegetation in Europe. Ecol. Indic. 158, 111486. https://doi.org/10.1016/j.ecolind.2023.111486.
Finch, D.P., Palmer, P.I., 2020. Increasing ambient surface ozone levels over the UK accompanied by fewer extreme events. Atmos. Environ. 237, 117627. https://doi.org/10.1016/j.atmosenv.2020.117627.
Forestry Statistics 2023: Chapter 1 - Woodland Area & Planting, 2023. Forest Research, Alice Holt.
Gäb, M., Hoffmann, K., Lobe, M., Metzger, R., van Ooyen, S., Elbers, G., Köllner, B., 2006. NIR-spectroscopic investigation of foliage of ozone-stressed Fagus sylvatica trees. J. For. Res. 11, 69–75. https://doi.org/10.1007/s10310-005-0186-3.
Gamon, J.A., Serrano, L., Surfus, J.S., 1997. The photochemical reflectance index: an optical indicator of photosynthetic radiation use efficiency across species, functional types, and nutrient levels. Oecologia 112, 492–501. https://doi.org/10.1007/s004420050337.
Gosselin, N., Sagan, V., Maimaitiyiming, M., Fishman, J., Belina, K., Podleski, A., Maimaitijiang, M., Bashir, A., Balakrishna, J., Dixon, A., 2020. Using visual ozone damage scores and spectroscopy to quantify soybean responses to background ozone. Remote Sens. 12, 93. https://doi.org/10.3390/rs12010093.
Grayson, A.J., Jones, E., 1956. Notes on the History of Wytham Estate with Special Reference to the Woodlands. Imperial Forestry Institute, Oxford.
Griffiths, P.T., Murray, L.T., Zeng, G., Shin, Y.M., Abraham, N.L., Archibald, A.T., Deushi, M., Emmons, L.K., Galbally, I.E., Hassler, B., Horowitz, L.W., Keeble, J., Liu, J., Moeini, O., Naik, V., O'Connor, F.M., Oshima, N., Tarasick, D., Tilmes, S., Turnock, S.T., Wild, O., Young, P.J., Zanis, P., 2021. Tropospheric ozone in CMIP6 simulations. Atmos. Chem. Phys. 21, 4187–4218. https://doi.org/10.5194/acp-21-4187-2021.
Guderian, R., 1985. Air Pollution by Photochemical Oxidants: Formation, Transport, Control, and Effects on Plants. Springer.
Harris, C.R., Millman, K.J., van der Walt, S.J., Gommers, R., Virtanen, P., Cournapeau, D., Wieser, E., Taylor, J., Berg, S., Smith, N.J., Kern, R., Picus, M., Hoyer, S., van Kerkwijk, M.H., Brett, M., Haldane, A., Fernández del Río, J., Wiebe, M., Peterson, P., Gérard-Marchant, P., Sheppard, K., Reddy, T., Weckesser, W., Abbasi, H., Gohlke, C., Oliphant, T.E., 2020. Array programming with NumPy. Nature 585, 357–362. https://doi.org/10.1038/s41586-020-2649-2.
Hart, K.M., Curioni, G., Blaen, P., Harper, N.J., Miles, P., Lewin, K.F., Nagy, J., Bannister, E.J., Cai, X.M., Thomas, R.M., Krause, S., Tausz, M., MacKenzie, A.R., 2020. Characteristics of free air carbon dioxide enrichment of a northern temperate mature forest. Glob. Change Biol. 26, 1023–1037. https://doi.org/10.1111/gcb.14786.
Hayes, F., Williamson, J., Mills, G., 2015. Species-specific responses to ozone and drought in six deciduous trees. Water. Air. Soil Pollut. 226, 156. https://doi.org/10.1007/s11270-015-2428-0.
Hill, A.C., Littlefield, N., 1969. Ozone. Effect on apparent photosynthesis, rate of transpiration, and stomatal closure in plants. Environ. Sci. Technol. 3, 52–56. https://doi.org/10.1021/es60024a002.
Hillstrom, M.L., Lindroth, R.L., 2008. Elevated atmospheric carbon dioxide and ozone alter forest insect abundance and community composition. Insect Conserv. Divers. 1, 233–241. https://doi.org/10.1111/j.1752-4598.2008.00031.x.
Hoshika, Y., Paoletti, E., Centritto, M., Gomes, M.T.G., Puértolas, J., Haworth, M., 2022. Species-specific variation of photosynthesis and mesophyll conductance to ozone and drought in three Mediterranean oaks. Physiol. Plant. 174, e13639. https://doi.org/10.1111/ppl.13639.
Hunter, J.D., 2007. Matplotlib: A 2D graphics environment. Comput. Sci. Eng. 9, 90–95.
IPCC, 2023. Climate Change 2021 – The Physical Science Basis: Working Group I Contribution to the Sixth Assessment Report of the Intergovernmental Panel on Climate Change. Cambridge University Press. https://doi.org/10.1017/9781009157896.
Kangasjärvi, J., Jaspers, P., Kollist, H., 2005. Signalling and cell death in ozone-exposed plants. Plant Cell Environ. 28, 1021–1036. https://doi.org/10.1111/j.1365-3040.2005.01325.x.
Kefauver, S.C., 2013. Using topographic and remotely sensed variables to assess ozone injury to conifers in the Sierra Nevada (USA) and Catalonia (Spain). Remote Sens. Environ. 11.
Kim, M.S., Mulchi, C.L., Daughtry, C.S.T., McMurtrey, J.E., 2004. Assessment of Combined Effects of Elevated Tropospheric O3 and CO2 on Soybean under Well-Watered and Restricted Soil Moisture Conditions by Multispectral Fluorescence Imaging Techniques, in: Digital Imaging and Spectral Techniques: Applications to Precision Agriculture and Crop Physiology. John Wiley & Sons, Ltd, pp. 223–253. https://doi.org/10.2134/asaspecpub66.c17.
Knudson, L.L., Tibbitts, T.W., Edwards, G.E., 1977. Measurement of ozone injury by determination of leaf chlorophyll concentration 1. Plant Physiol. 60, 606–608. https://doi.org/10.1104/pp.60.4.606.
Lee Jones, A., Ormondroyd, A., Hayes, F., Jeffers, E.S., 2024. Reflections of stress: ozone damage in broadleaf saplings can be identified from hyperspectral leaf reflectance. Environ. Pollut. 360, 124642. https://doi.org/10.1016/j.envpol.2024.124642.
Lee, Y., 2017. SpecDAL 2.0.0.
Lefohn, A.S., Malley, C.S., Smith, L., Wells, B., Hazucha, M., Simon, H., Naik, V., Mills, G., Schultz, M.G., Paoletti, E., De Marco, A., Xu, X., Zhang, L., Wang, T., Neufeld, H.S., Musselman, R.C., Tarasick, D., Brauer, M., Feng, Z., Tang, H., Kobayashi, K., Sicard, P., Solberg, S., Gerosa, G., 2018. Tropospheric ozone assessment report: global ozone metrics for climate change, human health, and crop/ecosystem research. Elem. Sci. Anthr. 6. https://doi.org/10.1525/elementa.279.
Li, P., Calatayud, V., Gao, F., Uddling, J., Feng, Z., 2016. Differences in ozone sensitivity among woody species are related to leaf morphology and antioxidant levels. Tree Physiol. 36, 1105–1116. https://doi.org/10.1093/treephys/tpw042.
Marchica, L., Cotrozzi, L., Nali, P., Remorini, 2019. Early detection of sage (Salvia officinalis L.) responses to ozone using reflectance spectroscopy. Plants 8, 346. https://doi.org/10.3390/plants8090346.
Marzuoli, R., Gerosa, G., Bussotti, F., Pollastrini, M., 2019. Assessing the impact of ozone on forest trees in an integrative perspective: are foliar visible symptoms suitable predictors for growth reduction? A critical review. Forests 10, 1144. https://doi.org/10.3390/f10121144.
Marzuoli, R., Monga, R., Finco, A., Gerosa, G., 2016. Biomass and physiological responses of Quercus robur (L.) young trees during 2 years of treatments with different levels of ozone and nitrogen wet deposition. Trees 30, 1995–2010. https://doi.org/10.1007/s00468-016-1427-0.
Mediavilla, S., Escudero, A., 2003. Mature trees versus seedlings: differences in leaf traits and gas exchange patterns in three co-occurring Mediterranean oaks. Ann. For. Sci. 60, 455–460. https://doi.org/10.1051/forest:2003038.
Meroni, M., Panigada, C., Rossini, M., Picchi, V., Cogliati, S., Colombo, R., 2009. Using optical remote sensing techniques to track the development of ozone-induced stress. Environ. Pollut. 157, 1413–1420. https://doi.org/10.1016/j.envpol.2008.09.018.
Meroni, M., Picchi, V., Rossini, M., Cogliati, S., Panigada, C., Nali, C., Lorenzini, G., Colombo, R., 2008a. Leaf level early assessment of ozone injuries by passive fluorescence and photochemical reflectance index. Int. J. Remote Sens. 29, 5409–5422. https://doi.org/10.1080/01431160802036292.
Meroni, M., Rossini, M., Picchi, V., Panigada, C., Cogliati, S., Nali, C., Colombo, R., 2008b. Assessing steady-state fluorescence and PRI from hyperspectral proximal sensing as early indicators of plant stress: the case of ozone exposure. Sensors 8, 1740–1754. https://doi.org/10.3390/s8031740.
Merzlyak, M.N., Gitelson, A.A., Chivkunova, O.B., Rakitin, V.Y.U., 1999. Non-destructive optical detection of pigment changes during leaf senescence and fruit ripening. Physiol. Plant. 106, 135–141. https://doi.org/10.1034/j.1399-3054.1999.106119.x.
Mevik, B.-H., Wehrens, R., 2007. The pls package: principal component and partial least squares regression in R. J. Stat. Softw. 18, 1–23. https://doi.org/10.18637/jss.v018.i02.
Mills, G., Harmens, H., Hayes, Felicity, Pleijel, H., Buker, P., González-Fernández, I., 2017. Chapter 3: Mapping critical levels for vegetation. ICP Vegetation.

Mills, G., Hayes, F., Simpson, D., Emberson, L., Norris, D., Harmens, H., Büker, P., 2011. Evidence of widespread effects of ozone on crops and (semi-)natural vegetation in Europe (1990–2006) in relation to AOT40- and flux-based risk maps. Glob. Change Biol. 17, 592–613. https://doi.org/10.1111/j.1365-2486.2010.02217.x.

Mitchell, R.J., Bellamy, P.E., Ellis, C.J., Hewison, R.L., Hodgetts, N.G., Iason, G.R., Littlewood, N.A., Newey, S., Stockan, J.A., Taylor, A.F.S., 2019. Collapsing foundations: the ecology of the British oak, implications of its decline and mitigation options. Biol. Conserv. 233, 316–327. https://doi.org/10.1016/j.biocon.2019.03.040.

Monks, P.S., Archibald, A.T., Colette, A., Cooper, O., Coyle, M., Derwent, R., Fowler, D., Granier, C., Law, K.S., Mills, G.E., Stevenson, D.S., Tarasova, O., Thouret, V., von Schneidemesser, E., Sommariva, R., Wild, O., Williams, M.L., 2015. Tropospheric ozone and its precursors from the urban to the global scale from air quality to short-lived climate forcer. Atmospheric Chem. Phys. 15, 8889–8973. https://doi.org/10.5194/acp-15-8889-2015.

Morecroft, M.D., Roberts, J.M., 1999. Photosynthesis and stomatal conductance of mature canopy Oak (Quercus robur) and Sycamore (Acer pseudoplatanus) trees throughout the growing season. Funct. Ecol. 13, 332–342. https://doi.org/10.1046/j.1365-2435.1999.00327.x.

Morecroft, M.D., Stokes, V.J., Taylor, M.E., Morison, J.I.L., 2008. Effects of climate and management history on the distribution and growth of sycamore (Acer pseudoplatanus L.) in a southern British woodland in comparison to native competitors. Forestry 81, 59–74. https://doi.org/10.1093/forestry/cpm045.

Moura, B.B., Paoletti, E., Badea, O., Ferrini, F., Hoshika, Y., 2022. Visible foliar injury and ecophysiological responses to ozone and drought in oak seedlings. Plants 11. https://doi.org/10.3390/plants11141836.

Norby, R.J., De Kauwe, M.G., Domingues, T.F., Duursma, R.A., Ellsworth, D.S., Goll, D.S., Lapola, D.M., Luus, K.A., MacKenzie, A.R., Medlyn, B.E., Pavlick, R., Rammig, A., Smith, B., Thomas, R., Thonicke, K., Walker, A.P., Yang, X., Zaehle, S., 2016. Model–data synthesis for the next generation of forest free-air CO_2 enrichment (FACE) experiments. New Phytol. 209, 17–28. https://doi.org/10.1111/nph.13593.

Norby, R.J., Loader, N.J., Mayoral, C., Ullah, S., Curioni, G., Smith, A.R., Reay, M.K., van Wijngaarden, K., Amjad, M.S., Brettle, D., Crockatt, M.E., Denny, G., Grzesik, R.T., Hamilton, R.L., Hart, K.M., Hartley, I.P., Jones, A.G., Kourmouli, A., Larsen, J.R., Shi, Z., Thomas, R.M., MacKenzie, A.R., 2024. Enhanced woody biomass production in a mature temperate forest under elevated CO_2. Nat. Clim. Change 14, 983–988. https://doi.org/10.1038/s41558-024-02090-3.

Nunn, A.J., Kozovits, A.R., Reiter, I.M., Heerdt, C., Leuchner, M., Lütz, C., Liu, X., Löw, M., Winkler, J.B., Grams, T.E.E., Häberle, K.-H., Werner, H., Fabian, P., Rennenberg, H., Matyssek, R., 2005. Comparison of ozone uptake and sensitivity between a phytotron study with young beech and a field experiment with adult beech (*Fagus sylvatica*). Environ. Pollut. 137, 494–506. https://doi.org/10.1016/j.envpol.2005.01.036.

O'Brien, L., Marzano, M., Dandy, N., Bates, S., Hemery, G., Petrokofsky, G., Dunn, M., Forster, J., 2024. Managing trees species of high social and cultural value: forest manager attitudes towards pest and disease risks to oak in Britain. Forests 15, 1695. https://doi.org/10.3390/f15101695.

Pellegrini, E., Hoshika, Y., Dusart, N., Cotrozzi, L., Gérard, J., Nali, C., Vaultier, M.-N., Jolivet, Y., Lorenzini, G., Paoletti, E., 2019. Antioxidative responses of three oak species under ozone and water stress conditions. Sci. Total Environ. 647, 390–399. https://doi.org/10.1016/j.scitotenv.2018.07.413.

Peñuelas, J., Filella, I., Gamon, J.A., 1995. Assessment of photosynthetic radiation-use efficiency with spectral reflectance. New Phytol. 131, 291–296. https://doi.org/10.1111/j.1469-8137.1995.tb03064.x.

Proietti, C., Anav, A., De Marco, A., Sicard, P., Vitale, M., 2016. A multi-sites analysis on the ozone effects on gross primary production of European forests. Sci. Total Environ. 556, 1–11. https://doi.org/10.1016/j.scitotenv.2016.02.187.

Proietti, C., Fornasier, M.F., Sicard, P., Anav, A., Paoletti, E., De Marco, A., 2021. Trends in tropospheric ozone concentrations and forest impact metrics in Europe over the time period 2000–2014. J. for. Res. 32, 543–551. https://doi.org/10.1007/s11676-020-01226-3.

Rouse, J.W., Haas, R.H., Schell, J.A., Deering, D.W., 1974. Monitoring vegetation systems in the Great Plains with ERTS. Presented at the NASA. Goddard Space Flight Center 3d ERTS-1 Symp., Vol. 1, Sect. A.

Ryalls, J.M.W., Bishop, J., Mofikoya, A.O., Bromfield, L.M., Nakagawa, S., Girling, R.D., 2024. Air pollution disproportionately impairs beneficial invertebrates: a meta-analysis. Nat. Commun. 15, 5447. https://doi.org/10.1038/s41467-024-49729-5.

Ryalls, J.M.W., Langford, B., Mullinger, N.J., Bromfield, L.M., Nemitz, E., Pfrang, C., Girling, R.D., 2022. Anthropogenic air pollutants reduce insect-mediated pollination services. Environ. Pollut. 297. https://doi.org/10.1016/j.envpol.2022.118847.

Sandermann Jr, H., 1996. Ozone and plant health. Annu. Rev. Phytopathol. 34, 347–366. https://doi.org/10.1146/annurev.phyto.34.1.347.

Sapes, G., Schroeder, L., Scott, A., Clark, I., Juzwik, J., Montgomery, R.A., Guzmán, Q.J. A., Cavender-Bares, J., 2024. Mechanistic links between physiology and spectral reflectance enable previsual detection of oak wilt and drought stress. Proc. Natl. Acad. Sci. 121, e2316164121. https://doi.org/10.1073/pnas.2316164121.

Schaub, M., Calatayud, V., Ferretti, M., Brunialti, G., Lövblad, G., Krause, G., Sanz, M.J., 2016. Part VIII: Monitoring of Ozone Injury., Manual on methods and criteria for harmonized sampling, assessment, monitoring and analysis of the effects of air pollution on forests. UNECE ICP Forests Programme Co-ordinating Centre, Thünen Institute of Forest Ecosystems.

Sharma, Y.K., Davis, K.R., 1997. The effects of ozone on antioxidant responses in plants. Free Radic. Biol. Med. 23, 480–488. https://doi.org/10.1016/S0891-5849(97)00108-1.

Sicard, P., De Marco, A., Dalstein-Richier, L., Tagliaferro, F., Renou, C., Paoletti, E., 2016. An epidemiological assessment of stomatal ozone flux-based critical levels for visible ozone injury in Southern European forests. Sci. Total Environ. 541, 729–741. https://doi.org/10.1016/j.scitotenv.2015.09.113.

Sicard, P., Vas, N., Calatayud, V., Garcia-Breijo, F.J., Reig-Armiñana, J., Sanz, M.J., Dalstein-Richier, L. 2010. Dommages forestiers et pollution à l'ozone dans les réserves naturelles : le cas de l'arolle dans le sud-est de la France -. For. Méditerranéenne XXXI, 273.

Sims, D.A., Gamon, J.A., 2002. Relationships between leaf pigment content and spectral reflectance across a wide range of species, leaf structures and developmental stages. Remote Sens. Environ. 81, 337–354. https://doi.org/10.1016/S0034-4257(02)00010-X.

Taylor, M.E., Morecroft, M.D., Oliver, H.R., 2011. The Physical Environment, in: Savill, P., Perrins, C., Kirby, K., Fisher, N. (Eds.), Wytham Woods: Oxford's Ecological Laboratory. Oxford University Press, p. 0. https://doi.org/10.1093/acprof:osobl/9780199605187.003.0002.

Taylor-Zavala, R., Ramírez-Rodríguez, O., de Armas-Ricard, M., Sanhueza, H., Higueras-Fredes, F., Mattar, C., 2021. Quantifying biochemical traits over the patagonian sub-antarctic forests and their relation to multispectral vegetation indices. Remote Sens. 13, 4232. https://doi.org/10.3390/rs13214232.

The Air Quality Limit Values Regulations 2003, n.d.

The National Emission Ceilings Regulations 2018, 2018.

Thomas, S.C., Winner, W.E., 2002. Photosynthetic differences between saplings and adult trees: an integration of field results by meta-analysis. Tree Physiol. 22, 117–127. https://doi.org/10.1093/treephys/22.2-3.117.

Treshow, M., 1970. Ozone damage to plants. Environ. Pollut. (1), 155–161. https://doi.org/10.1016/0013-9327(70)90016-9.

UK AIR, Department for Environment Food & Rural Affairs (DEFRA), 2023. Ozone AOT40 Modelled Background 2022.

Ustin, S.L., Curtiss, B., 1990. Spectral characteristics of ozone-treated conifers. Environ. Exp. Bot. 30, 293–308. https://doi.org/10.1016/0098-8472(90)90041-2.

Wessely, J., Essl, F., Fiedler, K., Gattringer, A., Hülber, B., Ignateva, O., Moser, D., Rammer, W., Dullinger, S., Seidl, R., 2024. A climate-induced tree species bottleneck for forest management in Europe. Nat. Ecol. Evol. 8, 1109–1117. https://doi.org/10.1038/s41559-024-02406-8.

Wittig, V.E., Ainsworth, E.A., Long, S.P., 2007. To what extent do current and projected increases in surface ozone affect photosynthesis and stomatal conductance of trees? A meta-analytic review of the last 3 decades of experiments. Plant Cell Environ. 30, 1150–1162. https://doi.org/10.1111/j.1365-3040.2007.01717.x.

Yang, X., Tang, J., Mustard, J.F., Wu, J., Zhao, K., Serbin, S., Lee, J.-E., 2016. Seasonal variability of multiple leaf traits captured by leaf spectroscopy at two temperate deciduous forests. Remote Sens. Environ. 179, 1–12. https://doi.org/10.1016/j.rse.2016.03.026.